Electronic Supplementary Material (ESI) for Analytical Methods.

Supplementary materials

Mixed hemi/ad-micelle SDS-coated magnetic $Fe_{2-x}Al_xO_3$ (x=0.4) nanoparticles for the capture of gatifloxacin and prulifloxacin coupled with fluorimetric determination

Juanli Du, Hao Wu*, Yu An, Yating Shi, Xiaozhen Guo, Liming Du*

School of Chemistry and Material Science, Shanxi Normal University, Shanxi Linfen, P.R. China 041004

*Corresponding author: Hao Wu

School of Chemistry and Material Science, Shanxi Normal University, Shanxi Linfen, P.R. China 041004

Tel.: +86 357 2057969

Fax: +86 357 2057969

E-mail: fxcszx@163.com

*Corresponding author: Liming Du

School of Chemistry and Material Science, Shanxi Normal University, Shanxi Linfen, P.R. China 041004

Tel.: +86 357 2057969

Fax: +86 357 2057969

E-mail: lmd@dns.sxnu.edu.cn

Apparatus

The Fe_3O_4 MNPs and $Fe_{2-x}Al_xO_3$ MNPs structural and morphological characterizations were carried out using Philips PW 3710 X-ray diffractometer with CrKα radiation. Transmission electron microscopy (TEM) measurements were carried out using a JEM-2100 at 100 kV machine. The energy dispersive X-ray analysis (EDAX) was investigated by scanning electron microscopy (SEM) coupled with an energy dispersive X-ray spectroscopy unit.

Characterization of the $Fe_{2-x}Al_xO_3$ MNPs

The adsorbents must possess superparamagnetic properties to achieve rapid separation under a magnetic field. Fig. S1 shows the magnetization curves for the Fe_3O_4 MNPs and $Fe_{2-x}Al_xO_3$ MNPs at room temperature. Both the Fe_3O_4 MNPs and $Fe_{2-x}Al_xO_3$ MNPs exhibit typical superparamagnetic behaviour due to the lack of hysteresis. The large saturation magnetization was 48.7 $emu \cdot g^{-1}$ for the $Fe_{2-x}Al_xO_3$ MNPs and 70.8 $emu \cdot g^{-1}$ for the Fe_3O_4 MNPs, which makes them very susceptible to magnetic fields. Fig. S2 shows the SEM image of the Fe_3O_4 MNPs and $Fe_{2-x}Al_xO_3$ MNPs, which illustrates the uniform size distribution of these nanoparticles. The diameter of the Fe_3O_4 MNPs was in the 40-50 nm range, and the diameter of the $Fe_{2-x}Al_xO_3$ MNPs was slightly larger. Therefore, the $Fe_{2-x}Al_xO_3$ MNPs leads to a decrease in the magnetic strength of Fe_3O_4 MNPs and an increase in the particle diameter of the Fe_3O_4 MNPs.

The crystal phases of Fe_3O_4 MNPs Al_2O_3 and $Fe_{2-x}Al_xO_3$ MNPs were compared using XRD, and the obtained XRD patterns are shown in Fig. S3. The diffraction pattern is in good agreement with the JCPDS file for Fe_3O_4, which indicated that the Fe_3O_4 nanoparticles are well cubic-crystals. For the $Fe_{2-x}Al_xO_3$ MNPs, a clear broad peak (at 45.7°, 70.2° and 73.6°)

corresponding to Fe_3O_4 can be observed. The results strongly suggest that Al was successfully doped into the Fe_3O_4 MNPs. The compositional analysis of the $Fe_{2-x}Al_xO_3$ MNPs was carried out with the aid of EDAX, which is shown in Fig. S4. Based on this study, the prepared MNPs are composites of Al, Fe and O.

Fig. S1 VSM magnetization curves of Fe_3O_4 MNPs and $Fe_{2-x}Al_xO_3$ MNPs.

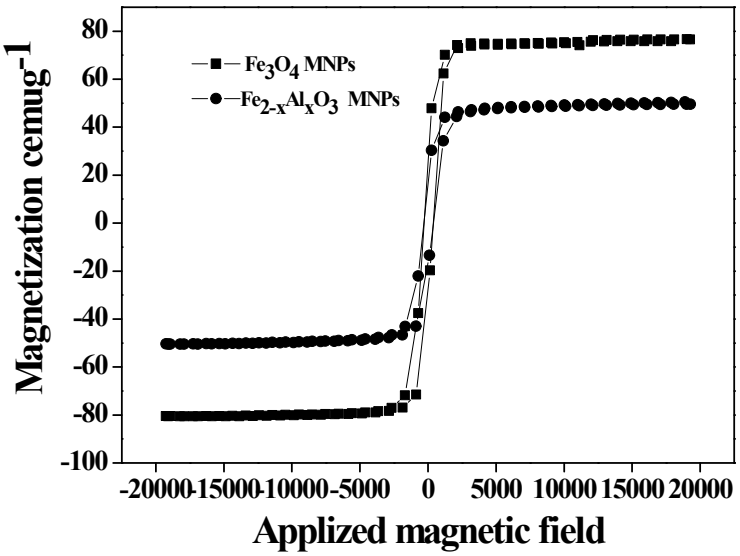

Fig. S2 SEM image of (a) Fe_3O_4 MNPs and (b) $Fe_{2-x}Al_xO_3$ MNPs.

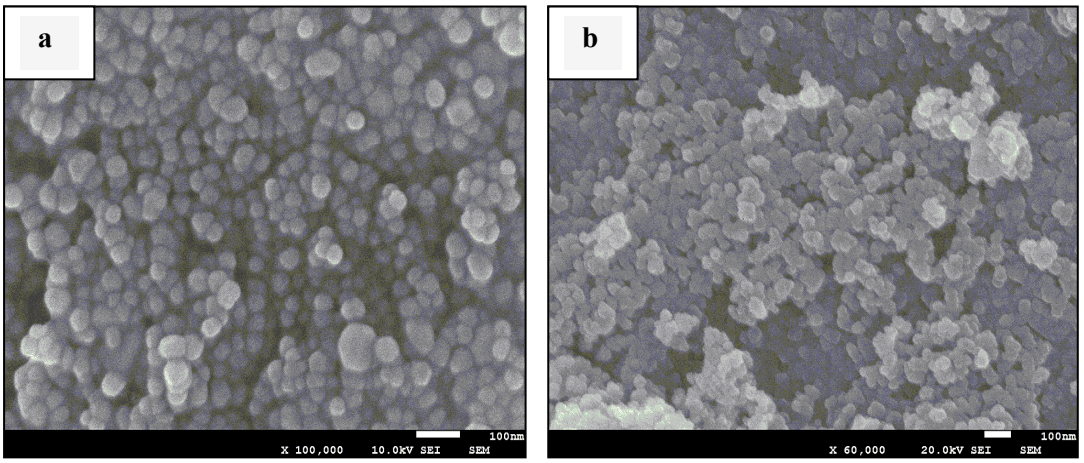

Fig. S3 XRD patterns of Fe_3O_4 MNPs and $Fe_{2-x}Al_xO_3$ MNPs.

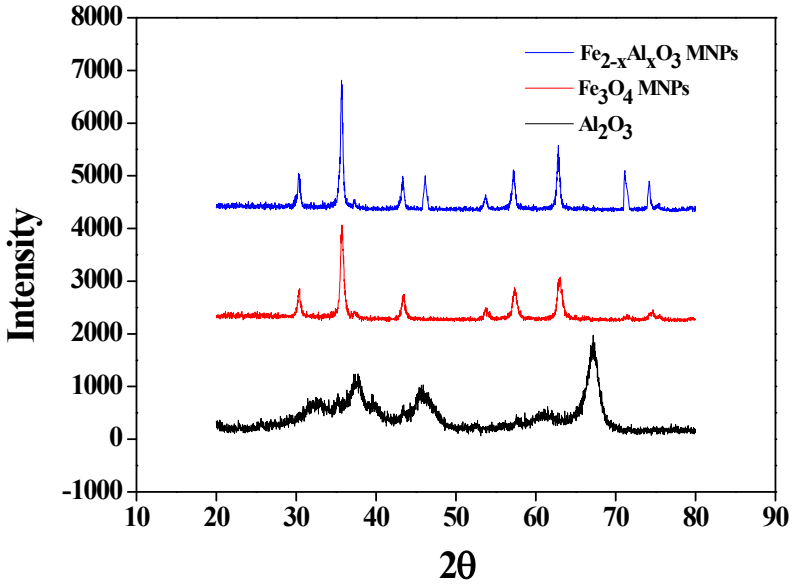

Fig. S4 EDAX spectrum of $Fe_{2-x}Al_xO_3$ MNPs.

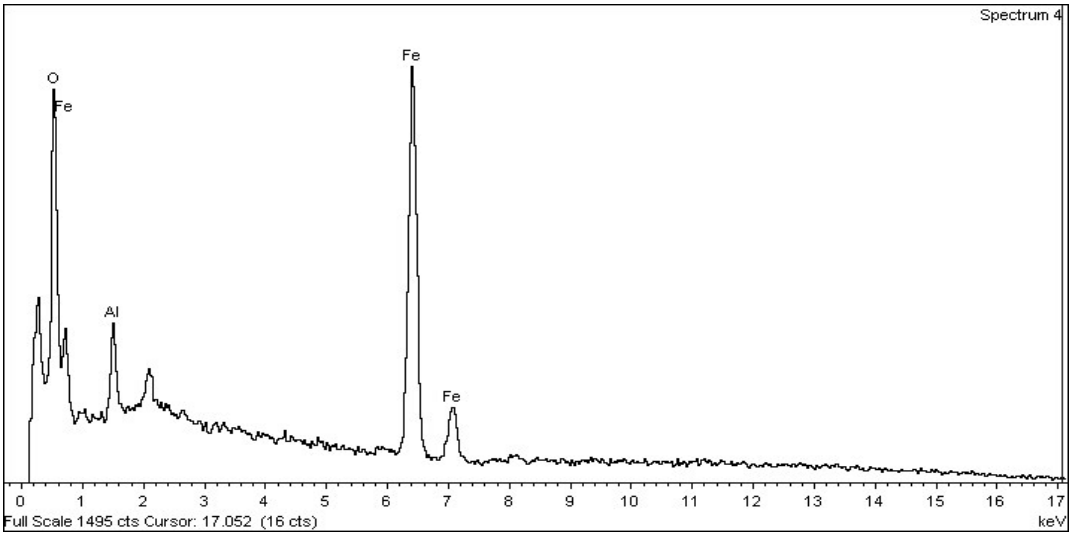

Fig. S5 Comparison of Fe_3O_4 MNPs and $Fe_{2-x}Al_xO_3$ MNPs. The extraction efficiency of $Fe_{2-x}Al_xO_3$ MNPs was better than that of Fe_3O_4 MNPs.

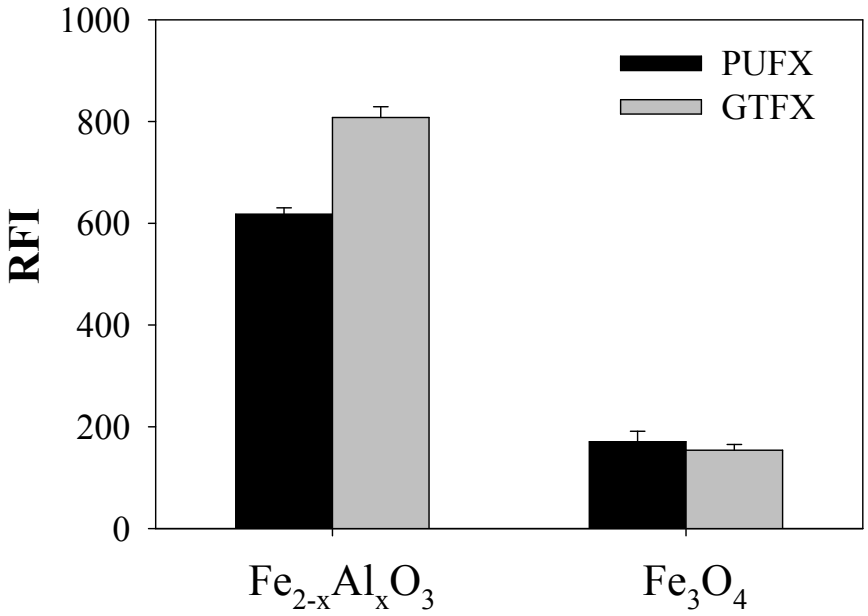

Fig. S6 Effect of the amount of NaCl. The amount of $Fe_{2-x}Al_xO_3$ MNPs was 8 mg or 15 mg, and 0.05-0.3 g of NaCl were added. Extraction conditions: SDS concentration, 40 $mg \cdot mL^{-1}$, extraction time, 8 min, desorption solvent volume 0.5 mL, desorption time, 7 min, sample pH 5.0 for GTFX and PUFX.